Exhibit C

MedicineNet.com
Smart Medicine



**Inflammation:** A basic way in which the body reacts to infection, irritation or other injury, the key feature being redness, warmth, swelling and pain. Inflammation is now recognized as a type of nonspecific immune response.

More information: In technical terms, the inflammatory response directs immune system components to the site of injury or infection and is manifest by increased blood supply and vascular permeability which, in technical terms, allows chemotactic peptides, neutrophils, and mononuclear cells to leave the intravascular compartment. Microorganisms are engulfed by phagocytic cells (e.g., neutrophils and macrophages) in an attempt to contain the infection in a small-tissue space. The response includes attraction of phagocytes in a chemotactic gradient of microbial products, movement of the phagocyte to the inflammatory site and contact with the organism, phagocytosis (ingestion) of the organism, development of an oxidative burst directed toward the organism, fusion of the phagosome and lysosome with degranulation of lysosomal contents, and death and degradation of the organism. When quantitative or qualitative defects in neutrophil function result in infection, the infection usually is prolonged and recurrent and responds slowly to antimicrobial agents. Staphylococci, gram-negative organisms, and fungi are the usual pathogens responsible for these infections.

History: Since antiquity (and to every medical student), the defining clinical features of inflammation have been known in Latin as rubor (redness), calor (warmth), tumor (swelling) and dolor (pain). These hallmarks of inflammation were first described by Celsus -- Aulus (Aurelius) Cornelius, a Roman physician and medical writer, who lived from about 30 B.C. to 45 A.D.

*Last Editorial Review: 11/19/00*

Exhibit A



Stroke

(*Stroke.* 1996;27:1657-1662.)




Articles

# Automated Measurement of Infarct Size With Scanned Images of Triphenyltetrazolium Chloride–Stained Rat Brains

Eric J. Goldlust, BS; Richard P. Paczynski, MD; Yong Y. He, MD; Chung Y. Hsu, MD, PhD; Mark P. Goldberg, MD

the Center for the Study of Nervous System Injury and Department of Neurology, Washington University School of Medicine, St Louis, Mo.

Correspondence to Mark P. Goldberg, MD, Department of Neurology, Box 8111, Washington University School of Medicine, 660 S Euclid Ave, St Louis, MO 63110. E-mail goldberg@neuro.wustl.edu.

## Abstract



*Background and Purpose* The extent of brain infarction after focal cerebral ischemia is frequently assessed with the mitochondrial activity indicator 2,3,5-triphenyltetrazolium chloride (TTC). We describe an automated procedure for analysis of infarct size in TTC-stained rat brains.

*Methods* Rats were subjected to middle cerebral artery occlusion and killed after 24 to 36 hours, and their brains were processed for TTC staining. Digital images of coronal sections from these brains (n>50) were acquired with a desktop color scanner. The resulting images were divided into red, blue, and green component images. Total brain and infarct areas were automatically determined on the basis of total pixel intensity and area after segmentation of the red and green images, respectively. Automated measurements were compared with those made with a video camera–based image acquisition system that required manual tracing of lesion boundaries.

*Results* The spatial resolution of scanned brain images (≈200 μm) was comparable to that of the

camera-based system and provided sufficient detail to recognize infarct boundaries and neuroanatomical features. Scanner-based acquisition and analysis were faster than with the camera-based method. The green component image accurately distinguished infarcted from normal brain, and the red component image represented total brain dimensions. Infarct measurements obtained by the automated method correlated closely with those from conventional apparatus ($R^2$=.89, $P$<.001). Intraobserver reliability with the automated method ($R^2$=1.00) was higher than with the conventional method ($R^2$=.77).

*Conclusions* Infarct size after middle cerebral artery occlusion in the rat can be rapidly and reproducibly assessed with inexpensive scanning equipment and automated image analysis of TTC-stained brains.

**Key Words:** cerebral infarction • diagnostic imaging • middle cerebral artery occlusion • rats

# Introduction



A common method of assessing lesion size in rat brains after transient focal ischemia involves staining the brains with 2,3,5-triphenyltetrazolium chloride (TTC).[1][2][3][4][5] TTC, which is itself colorless in solution, is reduced by enzymes of functioning mitochondria to yield a deep red formazan.[6][7] Infarcted brain regions do not convert TTC and remain unstained. TTC labeling demonstrates ischemic lesions that can be appreciated visually even without microscopic examination. Infarct areas measured with TTC correspond closely with those measured with other histological methods.[2][3][8][9] The robustness of this technique enables assessment of lesion size with minimal tissue preparation. Quantitative measurements of infarct volume determined in this manner have proven useful in determining the extent of brain injury in experimental stroke models and in assessing potential neuroprotective agents for cerebral ischemia.

Several investigators have described computer-assisted procedures to measure infarct areas with the use of brain sections stained with TTC[3][4][9][10][11][12] and other histological stains.[8][13][14][15][16][17] The most frequently used methods capture brain images with video cameras coupled to specialized image analysis systems, with cross-sectional areas automatically computed after manual tracing of the infarct boundaries. These techniques provide a quantitative assessment of infarct and total brain dimensions. However, they rely on relatively expensive dedicated equipment, and the manual cursor operation may be time-consuming and subjective. We sought to develop a more fully automated method for image acquisition and infarct measurement. Images are rapidly acquired with an inexpensive flatbed color scanner, and computer-based image analysis software is used to automatically recognize and measure infarct and total brain areas.

# Materials and Methods



### Perioperative Care and Surgical Procedures for Focal Ischemia

Twenty male Long-Evans rats weighing 300 to 350 g were used. All animal procedures were approved by the Animal Care Committee of Washington University Medical Center and fell within the guidelines for animal care established by the National Institutes of Health.

Animals were anesthetized with a single injection of chloral hydrate (400 mg/kg body wt IP). Body temperature (37±0.5°C) was maintained with a servo-controlled lamp connected to a rectal thermometer throughout surgery and until the recovery from anesthesia (return of righting reflexes). After recovery, animals were returned to their cages under ad libitum conditions.

Surgical procedures have been described in detail elsewhere.[18] Briefly, microsurgical techniques were used to expose the right middle cerebral artery. The middle cerebral artery was ligated at the level of the inferior cerebral vein with 10-0 ophthalmic suture. Both common carotid arteries were then exposed by a midline cervical incision and clamped with vascular clips. After the designated ischemic interval (60 to 90 minutes), the suture was removed from the middle cerebral artery, and the common carotid arteries were unclamped.

### TTC Staining

Twenty-four to 36 hours after atraumatic release of all three arteries, rats were deeply anesthetized with an injection of pentobarbital (70 mg/kg IP) and subjected to intracardiac perfusion with 100 mL of isotonic saline delivered through an electronic pump at 100 mm Hg. The head was then removed with a small animal guillotine and the brain carefully dissected out en bloc. After a brief (<1 minute) period of cooling on a bed of ice, the brain was sliced coronally at 2-mm intervals.

Individual slices were freed from dura mater and vascular tissue and soaked for 10 minutes in a solution of 2% TTC in 0.1 mol/L PBS (pH adjusted to 7.4), warmed to 37°C in a water bath. Gentle stirring of the slices ensured even exposure of the surfaces to staining. Excess TTC was then drained, and slices were refrigerated in 10% formalin.

### Spectrophotometry

Brains from rats subjected to middle cerebral artery occlusion were sectioned and stained, but not fixed, as described above. Samples of normal and infarcted tissue were isolated (29.6 mg), as was a sample of unstained, unfixed tissue from the same brain. Each section was placed in 1.00 mL of PBS and pulverized with a motorized centrifuge pellet pestle. The resulting suspension was scanned with a spectrophotometer (Beckman DU 650) to determine the absorbance of visible wavelengths from 400 to 700 nm.

### Scanner-Based Image Acquisition

Stained brains were stored between 1 and 11 days in a solution of 10% formalin in PBS and refrigerated at 4°C until the time of image processing. TTC staining intensity and image contrast diminished when brains were stored longer than 2 weeks. At that time, brain slices were separated, loose meningeal tissue was removed, and the brain stem was dissected away. A 150x15-mm Petri dish was placed on the scanning surface of a flatbed color scanner (ScanJet IIc, Hewlett-Packard) and filled with approximately 100 mL of 10% formalin. Coronal sections (2 mm) from up to five brains were submerged in formalin. Care was taken to ensure that sections did not come into contact with each other and that the flat edge of tissue surfaces remained in contact with the bottom of the Petri dish. Each slice was placed with its largest surface toward the scanner (ie, sections from the anterior half of the brain were imaged with the posterior surface down, and sections from the posterior half were imaged with the anterior surface down; the middle section was not imaged). This procedure ensured that the area of each coronal section was counted once.

The scanner was controlled with a PC-compatible computer with the provided software (DeskScan v2.2, Hewlett-Packard). The scanner lid was open to provide a blank background. The scanner was set to acquire 24-bit color images at 300 pixels per inch image resolution, with no color correction or image enhancement, and linear gain (gamma=1). The brightness setting (166) was set so that the background image was black (intensity=0). The contrast setting (182) was set so that the measured values did not exceed 255 for any color. The resulting image was saved as an uncompressed tagged image file format file and stored on magnetic or magneto-optical disk.

**Image Analysis and Infarct Size Determinations**

Images were processed on PC-compatible computers (486 or Pentium processors) with laboratory image analysis software (MetaMorph, Universal Imaging Corp), as diagrammed in Fig 1⊡. The color image was automatically partitioned into three monochrome images representing red, green, and blue components with pixel intensities ranging from 0 to 255. The red component image was thresholded with respect to gray level (pixel intensity >20) and segmented into discrete regions of contiguous pixels. Regions on the red image were classified as "total" brain regions if they had areas of 10 $mm^2$ or greater (≈139.5 pixels). Thresholding and segmentation were performed on the green component image to yield regions with gray values greater than 15. A region on the green image was classified as "infarct" if the sum of the gray levels of its component pixels was at least 7500. Region dimensions were converted from pixel areas to square millimeters on the basis of a calibration for the scanner resolution.

**Figure 1.** Algorithm for the automated method of infarct determination. See text for details. GV indicates gray value.

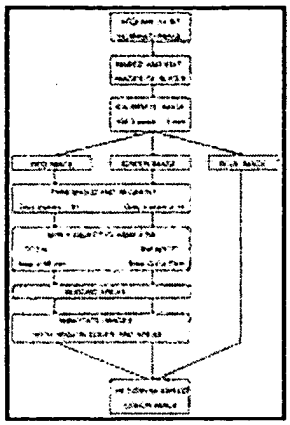

**View larger version** (23K):
[in this window]
[in a new window]

To display the measured contours, images consisting of infarct and total regions were generated in arbitrary colors on a black background, and the edges of such regions were determined by application of a Laplacian filter. These edges were superimposed onto the original color image. In addition, area measurements were overlayed on the image at the centroid of each region. This modified color image was displayed to confirm by visual inspection that regions of infarct and total brain had been determined in a manner similar to that of a human observer and to demonstrate the anatomic regions included within the infarct borders. Image thresholding, segmentation, region classification, unit conversion, measurement, edge detection, and related image processing were automated with the use of recorded keystroke sequences ("journals") in the MetaMorph image processing software. Supporting computer files designed for this experiment may be obtained from the authors.

Infarct measurements were also determined with an indirect method that compensates for edema of infarcted tissue. This method, described by Swanson et al[14] for Nissl-stained tissue, has been modified for measurement of TTC-stained tissue.[9] Indirect infarct measurements were calculated for each slice as Y=U-N+I, where Y is indirect infarct measurement, U is total area of the uninfarcted hemisphere, N is total area of the infarcted hemisphere, and I is area of the infarcted region (by direct measurement). For this analysis, the image was processed manually with a commercial image processing program (Photofinish, ZSoft) to bisect the image of each slice at the midline with a black line 2 pixels thick.

Some brain images required additional manual image editing. In cases in which lightly stained white matter or other tissue was immediately adjacent to infarct regions, the uninfarcted regions were masked by replacement with a solid red polygon. All alterations were retained in the computer image files for subsequent review.

**Comparison of Scanner-Based and Camera-Based Methods**

For manual infarct determination, brain slices were measured as previously described[10] [11] with a camera-based system. Briefly, images were acquired with a monochrome charge-coupled device (Sony) video camera with a 50 mm lens, digitized with a DUMAS image analysis system (Drexel University), and displayed on a color video monitor. The imaging software calculated infarct and total areas after region borders were manually delineated with a computer mouse.

Intraobserver reliability was assessed for both the scanner-based (automated) method and the camera-based (manual) method. In each case, a single observer (E.J.G.) reimaged the brains and performed measurements on two separate occasions.

Correlations between the scanner-based and camera-based methods were made by measuring the same surfaces of each slice by each method. These measurements were performed by different observers blinded to the other's results.

Linear regression was used to determine the relationship between area measurements performed by different observers or techniques. Correlation coefficients (Pearson's product moment correlation) and paired *t* tests were computed with SigmaStat software (Jandel Scientific).

# Results


- Top
- Abstract
- Introduction
- Materials and Methods
- Results
- Discussion
- References
- Introduction


### Spectrophotometry

Compared with infarcted tissue, uninfarcted brain stained with TTC selectively absorbed light at blue and green wavelengths (peak, ≈510 nm) but not red wavelengths (>620 nm) (Fig 2). The absorbance spectra of infarcted regions of TTC-stained brain were similar to those of unstained brain. Therefore, absorbance of green light distinguished TTC-stained infarcted and uninfarcted tissue.

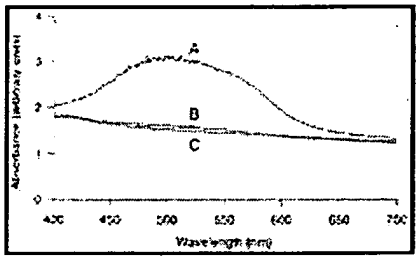


**View larger version** (12K):
[in this window]
[in a new window]

**Figure 2.** The absorbance spectrum of 2,3,5-triphenyltetrazolium chloride–stained (infarcted and uninfarcted) and unstained rat brain (in suspension in PBS). Reported absorbance values are proportional to the logarithm of the transmittance. Line A represents stained, uninfarcted tissue; line B represents stained, infarcted tissue; and line C represents unstained tissue.

### Scanner-Based Image Acquisition

When we used an optical test pattern (Edmund Scientific), the optical resolution of the scanner (at

400 pixels per inch, the highest setting) and that of the video camera (with 50-mm lens) were both approximately 200 µm. Scanner measurements of a 17x17-mm gray test specimen yielded uniform brightness values across the scanner surface.

Scanned images of TTC-stained sections provided high spatial resolution and allowed observation of brain morphology. Color images demonstrated both infarcted areas and normal brain (Fig 3A). Infarct borders were less readily distinguished when the same brain sections were scanned with monochrome settings or when images were acquired with the monochrome camera. For quantitative image analysis, the color image was split into red, green, and blue component images. The red component image enhanced the distinction between gray and white matter, permitting inspection of brain morphology and anatomic landmarks (Fig 3B). The green component image provided markedly enhanced contrast between infarcted (bright) and uninfarcted (dark) brain regions (Fig 3C). These observations are consistent with the spectrophotometric data, in that the green component image (corresponding to absorbance of green light) provided the best demarcation between infarcted and uninfarcted TTC-stained brain.

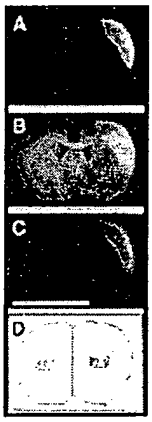


**View larger version** (36K): [in this window] [in a new window]

**Figure 3.** The transformation of a brain section image processed according to the algorithm in Fig 1. The rat brain was stained with 2,3,5-triphenyltetrazolium chloride 24 to 36 hours after right middle cerebral artery occlusion. A 2-mm coronal section at the level of the bregma is shown. A, Color image of brain as scanned. This 210x145 pixel image is a subset of a larger image file with several brains processed together. B, Red component image, used to measure total brain area and to assess anatomic landmarks. The brightness of each pixel represents the intensity of red light sampled from brain tissue. Note enhanced contrast between gray and white matter compared with color image. C, Green component image, used to distinguish infarct (white) from normal brain or background (black). D, Infarct (green) and total (red) left and right hemisphere regions delineated by image processing. Values represent measured areas in square millimeters. In practice, image D is overlaid onto image A or B to verify the accuracy of the computer-generated tracings. Scale bar=10 mm.

**Automated Analysis of Infarct and Total Areas**

Image analysis resulted in accurate determination of measured regions of infarcted and total brain (Fig 3D). The automated tracings acquired from the red image delineated areas of total brain tissue (ie, distinguished brain tissue from background), and tracings from the green image delineated areas of infarcted tissue only (ie, distinguished infarcted brain tissue from both background and uninfarcted tissue). The automated method was therefore reliable in distinguishing between infarcted brain tissue, uninfarcted brain tissue, and background. Measurement of pixel intensities on the green images provided information that was not apparent on visual inspection of the stained brain sections. Infarct borders demarcated by TTC staining were not always abrupt but could be graded over a distance of 0.8 to 1.5 mm (see Fig 3C,

medial top border of infarct). In addition, white matter adjacent to infarcted cortex often showed reduced TTC staining compared with control or contralateral tissue.

### Intraobserver Reliability and Correlation Between Scanner-Based and Camera-Based Measurements

Direct (I) and indirect (U-N+I) infarct measurements of the same slices determined by the automated system were consistent between repeated sessions (Fig 4A and 4B⊞): direct measurements, $R^2$=1.00 (n=50, $P$<.001); indirect measurements, $R^2$=.85 (n=50, $P$<.001). Similar measurements were less reproducible for the camera-based method (Fig 4C and 4D⊞): direct infarct, $R^2$=.77 (n=54, $P$<.001); indirect infarct, $R^2$=.57 (n=54, $P$<.001).

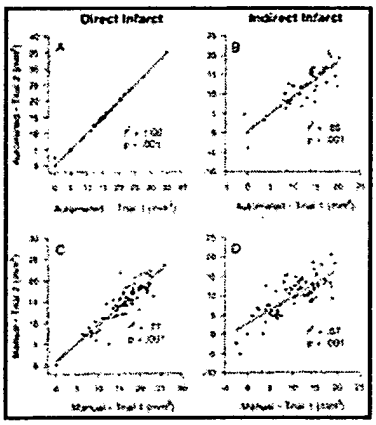


**View larger version** (28K):
[in this window]
[in a new window]

**Figure 4.** Intraobserver reliability of automated and manual methods of infarct measurement. Data points represent infarct areas of single slices, and solid lines indicate first-order linear regressions. For all data sets, multiple data points may be superimposed at the origin and other points. A, Direct infarct measurement (I) by the automated method; B, indirect infarct (U-N+I; see text) by the automated method; C, direct infarct measurement by the manual method; D, indirect infarct by the manual method. Measurements for A and B were taken by the same observer within 4 hours (n=50). Measurements for C and D were taken by the same observer within 24 hours (n=73). The indirect procedure for measuring infarct area (B and D) sometimes yielded negative values, reflecting asymmetries in the measured areas of the two hemispheres.

Area determinations by the camera-based and scanner-based methods were well correlated ($R^2$>.8, $P$<.001 for all comparisons; Fig 5⊞). The automated method generated slightly larger mean areas than the camera method for each measurement. The mean difference for infarcts by the direct method was 2.83±4.26 mm$^2$ ($P$<.001, n=54) compared with 1.64±5.57 mm$^2$ ($P$<.05, n=54) for infarcts by the indirect method and 8.62±7.47 mm$^2$ ($P$<.001, n=51) for total areas.

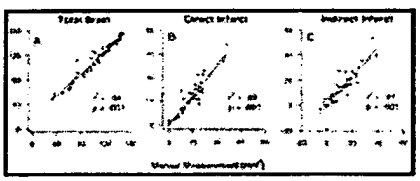

**View larger version** (14K):
[in this window]
[in a new window]

**Figure 5.** Correlation between infarct measurements by automated and manual methods. Data points represent region areas of single slices, solid lines represent first-order linear regression, and dotted lines represent the identity function ($y$=$x$). For all data sets, multiple data points may be superimposed at the origin and other points. A, Total area (U+N; see text; n=51); B, direct infarct measurement (I; n=54); C, indirect infarct measurement (U-N+I; n=54). The indirect procedure for measuring infarct area sometimes yielded negative values, reflecting asymmetries in the measured areas of

the two hemispheres.

## Discussion

Top
Abstract
Introduction
Materials and Methods
Results
Discussion
References
Introduction

The reliability of TTC in distinguishing infarcted from uninfarcted brain regions has been established in several models of focal ischemia.[3,4,5,11] Our method of infarct measurement has two novel components. First, an inexpensive flatbed scanner was used for image acquisition. The scanner's optical resolution (≈200 μm) was sufficient to distinguish brain morphological features. An important practical advantage of the scanner was its much larger field of acquisition. A typical flatbed scanner has a field of 22.5x36.5 cm (2655x4307 pixels at 118 pixels per centimeter) and thus can acquire full-color data at high resolution from all sections of several brains at once; the maximum acquisition is determined only by file size limitations of the image processing software. In addition, the scanner provided uniform illumination across the field of acquisition. In contrast, typical video camera–based acquisition devices with a constant image size of 512x480 pixels are limited to a much smaller field at the same resolution (4.3x4.1 cm) and can capture only a few slices in one image. Therefore, color desktop scanners are preferable to dedicated video acquisition systems for image acquisition in this application.

The second component of this technique is the method of automated image processing. A limitation of common methods for measuring TTC-stained brains is that they require subjective definition of lesion boundaries in each specimen, which may introduce observer bias and interobserver variability. Some histological stains distinguish infarct regions clearly enough to allow automated measurement based on pixel intensities.[14] However, we found that monochrome images of TTC-stained brains did not provide an optimal distinction between infarcted and normal tissue (particularly white matter). Spectral analysis indicated that TTC-stained uninfarcted brain regions selectively absorbed green light, which suggested that measured absorbance of green light could be exploited to delineate infarcted from uninfarcted regions. Partitioning color images into red and green components improved visualization of normal anatomy (red component image) and greatly enhanced definition of infarct areas (green component image), such that automated measurements were possible with little further computation. In the present method, infarct regions were determined by applying a gray-level threshold, grouping contiguous pixels, and classifying as infarct those regions that met certain size and intensity criteria. This simple image analysis procedure did not depend on the method of image acquisition and could be applied to video acquisition with the use of a color camera or a monochrome camera equipped with a green filter.

Infarct measurements in which automated methods were used were reproducible (Fig 4) and correlated well between manual and automated methods (Fig 5). An important feature of the image processing system used in these experiments was the ability to verify automated detected

contours by superimposing their outlines on the original image.

The automated procedure in which scanner acquisition was used was much faster than a conventional manual method. Acquisition and analysis of infarct areas from six to 10 brains (36 to 60 sections) could be completed in less than an hour; the longest step was orienting the brain sections on the imaging surface. Infarct measurements by manual tracing of sequential brain sections required approximately 45 minutes per brain.

Automated infarct analysis was not without limitations. The automated procedure was more sensitive to variations in histological processing and in the intensity and uniformity of TTC staining. Because the intensity of TTC staining decreased over time, it was necessary to acquire images for automated analysis within a few days of staining. Staining intensity was particularly critical in the present stroke model, in which infarcted gray matter bordered on intact white matter tracts, which were less deeply stained by TTC. In the case of poorly stained brain sections, human observers could distinguish adjacent regions of normal white matter from infarct regions, but the automated method sometimes required additional image editing to make this separation (this occurred in 13 of 154 brain section images included in Figs 4 and 5). Manual image editing was also required to bisect coronal sections for infarct measurements determined by the indirect method. Unlike human observers, the image analysis system was unable to exclude the edges of thick sections when these edges appeared in the scanned image. This problem may be addressed by preparation of thinner sections. Alternatively, since each coronal section is represented by the two opposing surfaces of adjacent slices, we avoided the problem by scanning only the largest side of each slice. This does not alter the determination of brain infarct volume, which is calculated by multiplying cross-sectional areas by the slice thickness (2 mm). Finally, the TTC method itself may have disadvantages, independent of the lesion measurement technique. The all-or-none measurement of impaired mitochondrial function is not specific for cell death and does not offer the level of cellular detail provided by histological examination of lesioned tissue.

Despite potential limitations, this method offers many advantages compared with dedicated camera-based image acquisition systems. Both image acquisition and image analysis are rapid and reproducible. The equipment is already present in some laboratories and is relatively inexpensive: desktop scanners and basic image analysis software packages are each available for less than $500. While the present technique yields an all-or-none discrimination between infarcted and normal tissue, these methods are readily extended to provide continuous measures of staining intensity. Such data might be useful for assessing graded lesions, examining other histological stains or indicators, or preparing data for quantitative analysis.

## Acknowledgments

This study was supported by National Institutes of Health grants NS32636 (Drs Hsu and Goldberg), NS01543 (Dr Goldberg), NS25545 (Dr Hsu), and NS28995 (Dr Hsu) and by National

Stroke Association career development award 38492 (Dr Paczynski). This research was done during the tenure of a Grant-in-Aid Award (to Dr Goldberg) from the American Heart Association and William Randolph Hearst Foundation. We thank Christine Leung for participating in the development of methods and Amol Shrikhande for assisting with manual infarct measurements.

Received March 28, 1996; revision received May 15, 1996; accepted May 16, 1996.

## References

Top
Abstract
Introduction
Materials and Methods
Results
Discussion
References
Introduction

1. Liszczak TM, Hedley-Whyte ET, Adams JF, Han DH, Kolluri VS, Vacanti FX, Heros RC, Zervas NT. Limitations of tetrazolium salts in delineating infarcted brain. *Acta Neuropathol (Berl).* 1984;65:150-157.[Medline]
2. Lundy EF, Solik BS, Frank RS, Lacy PS, Combs DJ, Zelenock GB, D'Alecy LG. Morphometric evaluation of brain infarcts in rats and gerbils. *J Pharmacol Methods.* 1986;16:201-214.[Medline]
3. Bederson JB, Pitts LH, Germano SM, Nishimura MC, Davis RL, Bartkowski HM. Evaluation of 2,3,5-triphenyltetrazolium chloride as a stain for detection and quantification of experimental cerebral infarction in rats. *Stroke.* 1986;17:1304-1308.[Abstract]
4. Park CK, Mendelow AD, Graham DI, McCulloch J, Teasdale GM. Correlation of triphenyltetrazolium chloride perfusion staining with conventional neurohistology in the detection of early brain ischaemia. *Neuropathol Appl Neurobiol.* 1988;14:289-298. [Medline]
5. Hatfield RH, Mendelow AD, Perry RH, Alvarez LM, Modha P. Triphenyltetrazolium chloride (TTC) as a marker for ischaemic changes in rat brain following permanent middle cerebral artery occlusion. *Neuropathol Appl Neurobiol.* 1991;17:61-67.[Medline]
6. Nachlas MM, Tson KC, Souza ED, Chang CS, Seligman AM. Cytochemical demonstration of succinic dehydrogenase by the use of a new p-nitrophenyl substituted ditetrazole. *J Histochem Cytochem.* 1957;5:420-436.
7. Altman FP. Tetrazolium salts and formazans. *Prog Histochem Cytochem.* 1976;9:1-56. [Medline]
8. Osborne KA, Shigeno T, Balarsky AM, Ford I, McCulloch J, Teasdale GM, Graham DI. Quantitative assessment of early brain damage in a rat model of focal cerebral ischaemia. *J Neurol Neurosurg Psychiatry.* 1987;50:402-410.[Abstract]
9. Lin TN, He YY, Wu G, Khan M, Hsu CY. Effect of brain edema on infarct volume in a focal cerebral ischemia model in rats. *Stroke.* 1993;24:117-121.[Abstract]
10. Chen ST, Hsu CY, Hogan EL, Juan HY, Banik NL, Balentine JD. Brain calcium content in ischemic infarction. *Neurology.* 1987;37:1227-1229.[Abstract]
11. Liu TH, Beckman JS, Freeman BA, Hogan EL, Hsu CY. Polyethylene glycol-conjugated superoxide dismutase and catalase reduce ischemic brain injury. *Am J Physiol.* 1989;256:589-593.
12. Aronowski J, Ostrow P, Samways E, Strong R, Zivin JA, Grotta JC. Graded bioassay for demonstration of brain rescue from experimental acute ischemia in rats. *Stroke.* 1994;25:2235-2240.[Abstract]
13. Jones PG, Coyle P. Microcomputer assisted lesion size measurements in spontaneously hypertensive stroke-prone rats. *J Electrophysiol Tech.* 1984;11:71-78.

14. Swanson RA, Morton MT, Tsao Wu G, Savalos RA, Davidson C, Sharp FR. A semiautomated method for measuring brain infarct volume. *J Cereb Blood Flow Metab.* 1990;10:290-293.[Medline]
15. Jacewicz M, Tanabe J, Pulsinelli WA. The CBF threshold and dynamics for focal cerebral infarction in spontaneously hypertensive rats. *J Cereb Blood Flow Metab.* 1992;12:359-370.[Medline]
16. Memezawa H, Minamisawa H, Smith ML, Siesjo BK. Ischemic penumbra in a model of reversible middle cerebral artery occlusion in the rat. *Exp Brain Res.* 1992;89:67-78.[Medline]
17. Zhao W, Ginsberg MD, Smith DW. Three-dimensional quantitative autoradiography by disparity analysis: theory and application to image averaging of local cerebral glucose utilization. *J Cereb Blood Flow Metab.* 1995;15:552-565.[Medline]
18. Chen ST, Hsu CY, Hogan EL, Maricq H, Balentine JD. A model of focal ischemic stroke in the rat: reproducible extensive cortical infarction. *Stroke.* 1986;17:738-743.[Abstract]

# Editorial Comment

Marc Fisher, MD, *Guest Editor*

The Medical Center of Central MassachusettsWorcester, Mass

## Introduction



The accurate measurement of postmortem infarct size is a key and basic element in many experimental focal ischemia studies. The use of 2,3,5-triphenyltetrazolium chloride (TTC) staining of mitochondrial activity to identify infarcted regions is now widely used and is well correlated with more traditional staining procedures. Most investigators use an image analysis system with a manual cursor to distinguish between red-stained normal tissue and nonstained infarcted tissue. This method requires an initial investment to acquire the necessary equipment and is potentially prone to interobserver variability.

In this interesting and innovative study, Goldlust and colleagues introduce an automated approach to defining infarct size by using an automated scanner-based image analysis system in comparison with the manual camera-based system. As the figures demonstrate, the color absorbance approach readily distinguished normal and infarcted brain. The automated infarct analysis was reproducible and well correlated with the traditional method. This advance in the identification of TTC-derived infarction will likely be widely used by other investigators, and the Washington University group should be congratulated for another important contribution to stroke modeling.

# This article has been cited by other articles:

Journal of Histochemistry & Cytochemistry ▸HOME

K. A. Matkowskyj, R. Cox, R. T. Jensen, and R. V. Benya
**Quantitative Immunohistochemistry by Measuring Cumulative Signal Strength Accurately Measures Receptor Number**
J. Histochem. Cytochem., February 1, 2003; 51(2): 205 - 214.
[Abstract] [Full Text] [PDF]

---

JVIR ▸HOME

M. Ahmed, S. M. Lobo, J. Weinstein, J. B. Kruskal, G. S. Gazelle, E. F. Halpern, S. K. Afzal, R. E. Lenkinski, and S. N. Goldberg
**Improved Coagulation with Saline Solution Pretreatment during Radiofrequency Tumor Ablation in a Canine Model**
J. Vasc. Interv. Radiol., July 1, 2002; 13(7): 717 - 724.
[Abstract] [Full Text] [PDF]

---

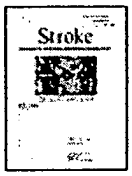

Stroke ▸HOME

S.-P. Lin, S.-K. Song, J. P. Miller, J. J.H. Ackerman, and J. J. Neil
**Direct, Longitudinal Comparison of 1H and 23Na MRI After Transient Focal Cerebral Ischemia**
Stroke, April 1, 2001; 32(4): 925 - 932.
[Abstract] [Full Text]

---

*Radiology* ▸HOME

S. N. Goldberg, M. Ahmed, G. S. Gazelle, J. B. Kruskal, J. C. Huertas, E. F. Halpern, B. S. Oliver, and R. E. Lenkinski
**Radio-Frequency Thermal Ablation with NaCl Solution Injection: Effect of Electrical Conductivity on Tissue Heating and Coagulation--Phantom and Porcine Liver Study**
Radiology, April 1, 2001; 219(1): 157 - 165.
[Abstract] [Full Text]

---

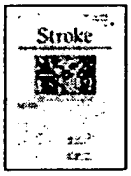

Stroke ▸HOME

A. Majid, Y. Y. He, J. M. Gidday, S. S. Kaplan, E. R. Gonzales, T. S. Park, J. D. Fenstermacher, L. Wei, D. W. Choi, C. Y. Hsu, and P. H. Chan
**Differences in Vulnerability to Permanent Focal Cerebral Ischemia Among 3 Common Mouse Strains Editorial Comment**
Stroke, November 1, 2000; 31(11): 2707 - 2714.
[Abstract] [Full Text] [PDF]

---

Journal of Histochemistry & Cytochemistry ▸HOME

K. A. Matkowskyj, D. Schonfeld, and R. V. Benya
**Quantitative Immunohistochemistry by Measuring Cumulative Signal Strength Using Commercially Available Software Photoshop and Matlab**
J. Histochem. Cytochem., February 1, 2000; 48(2): 303 - 312.
[Abstract] [Full Text]

---

Radiology HOME

S. N. Goldberg, R. C. Walovitch, J. A. Straub, M. T. Shore, and G. S. Gazelle

**Radio-frequency-induced Coagulation Necrosis in Rabbits: Immediate Detection at US with a Synthetic Microsphere Contrast Agent**

Radiology, November 1, 1999; 213(2): 438 - 444.

[Abstract] [Full Text]

---

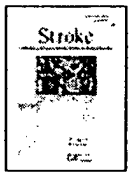

Stroke HOME

J. Vogel, C. Mobius, W. Kuschinsky, and W. I. Rosenblum

**Early Delineation of Ischemic Tissue in Rat Brain Cryosections by High-Contrast Staining • Editorial Comment**

Stroke, May 1, 1999; 30(5): 1134 - 1141.

[Abstract] [Full Text] [PDF]

---

Journal of Histochemistry & Cytochemistry HOME

H.-A. Lehr, C. M. van der Loos, P. Teeling, and A. M. Gown

**Complete Chromogen Separation and Analysis in Double Immunohistochemical Stains Using Photoshop-based Image Analysis**

J. Histochem. Cytochem., January 1, 1999; 47(1): 119 - 126.

[Abstract] [Full Text]

---

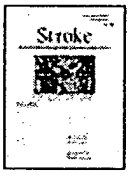

Stroke HOME

C. G. Markgraf, N. L. Velayo, M. P. Johnson, D. R. McCarty, S. Medhi, J. R. Koehl, P. A. Chmielewski, M. D. Linnik, and J. A. Clemens

**Six-Hour Window of Opportunity for Calpain Inhibition in Focal Cerebral Ischemia in Rats • Editorial Comment**

Stroke, January 1, 1998; 29(1): 152 - 158.

[Abstract] [Full Text] [PDF]

---